ORIGINAL RESEARCH

Impaired Development of Left Anterior Heart Field by Ectopic Retinoic Acid Causes Transposition of the Great Arteries

Mayu Narematsu; Tatsuya Kamimura, MS; Toshiyuki Yamagishi, PhD; Mitsuru Fukui, PhD; Yuji Nakajima, MD, PhD

***Background*—**Transposition of the great arteries is one of the most commonly diagnosed conotruncal heart defects at birth, but its etiology is largely unknown. The anterior heart field (AHF) that resides in the anterior pharyngeal arches contributes to conotruncal development, during which heart progenitors that originated from the left and right AHF migrate to form distinct conotruncal regions. The aim of this study is to identify abnormal AHF development that causes the morphology of transposition of the great arteries.

***Methods and Results*—**We placed a retinoic acid–soaked bead on the left or the right or on both sides of the AHF of stage 12 to 14 chick embryos and examined the conotruncal heart defect at stage 34. Transposition of the great arteries was diagnosed at high incidence in embryos for which a retinoic acid–soaked bead had been placed in the left AHF at stage 12. Fluorescent dye tracing showed that AHF exposed to retinoic acid failed to contribute to conotruncus development. FGF8 and Isl1 expression were downregulated in retinoic acid–exposed AHF, and differentiation and expansion of cardiomyocytes were suppressed in cultured AHF in medium supplemented with retinoic acid.

***Conclusions*—**The left AHF at the early looped heart stage, corresponding to Carnegie stages 10 to 11 (28 to 29 days after fertilization) in human embryos, is the region of the impediment that causes the morphology of transposition of the great arteries.
(*J Am Heart Assoc*. 2015;4:e001889 doi: 10.1161/JAHA.115.001889)

Key Words: congenital • heart defects • Isl1 • morphogenesis • transposition of great vessel

Congenital heart defects are among the most common congenital anomalies diagnosed at birth, and severe forms of congenital heart defect often require heart surgery during the neonatal to infant period. Congenital heart defects occur in ≈1% of live births.[1] Transposition of the great arteries (TGA) is one of the most common cyanotic congenital heart defects diagnosed at birth, constituting ≈5% of all congenital heart defects and 34% of situs solitus conotruncal heart defects.[2] The most characteristic anatomical feature of TGA, involving the aorta being right ventrally transposed to the pulmonary trunk, results in a connection between the right ventricle and the systemic channel. In normal heart, the pulmonary trunk is located on the left ventral side of the aorta, thereby establishing a normal ventricle-to-arterial connection, which is required for a series circuit of systemic and pulmonary circulation.

Two main morphological mechanisms leading to TGA have been concisely reviewed.[3] The first is the lack of counterclockwise rotation of the conotruncus (outflow tract [OFT]; viewed from the apex), which means that the right ventrally developed systemic channel fails to connect with the left ventricle. The second is abnormal conotruncal septation, by which conotruncal ridges fail to form the spirally oriented ventricle-to-arterial route, resulting in the parallel orientation of right ventral systemic and left dorsal pulmonary channels. Both of these theories are plausible because experimental models showed a rotational defect of conotruncus and straight conotruncal septation in the developing OFT directing TGA morphology.[4–9] Although several mutant mice have been reported to be associated with conotruncal defects including TGA, the molecular, cellular, and morphological etiologies causing TGA are largely unclear.[10]

At the beginning of this century, it was rediscovered that the myocardium of the OFT and right ventricle is added to the arterial pole of the heart tube from the mesodermal core of

From the Department of Anatomy and Cell Biology (M.N., T.K., T.Y., Y.N.) and Laboratory of Statics (M.F.), Graduate School of Medicine, Osaka City University, Osaka, Japan.

Accompanying Figures S1 through S9 and Table S1 are available at http://jaha.ahajournals.org/content/4/5/e001889/suppl/DC1

Correspondence to: Yuji Nakajima, MD, PhD, Department of Anatomy and Cell Biology, Graduate School of Medicine, Osaka City University, 1-4-3 Asahimachi, Abenoku, Osaka 545-8585, Japan. E-mail: yuji@med.osaka-cu.ac.jp

Received February 9, 2015; accepted April 3, 2015.

anterior pharyngeal arches and splanchnic mesoderm of the pericardial coelom dorsal to the OFT. Such heart-forming regions are respectively identified as an anterior heart field (AHF) and a secondary heart field (SHF) in chick embryos.[11,12] In the case of mouse, *Fgf10*-expressing pharyngeal mesoderm is reported to contribute to form conotruncus and right ventricle.[13] During the addition of cardiomyocytes to the developing OFT, its elongation and rotation are essential not only for normal septation of the conotruncus but also for establishment of a concordant ventriculoarterial connection. We previously reported that myocardial progenitor cells derived from left or right AHF (or SHF) generate distinct conotruncal regions.[14] This observation suggests that the impediment of AHF or SHF may cause a specific spectrum of conotruncal heart defects.[15]

Retinoic acid (RA), an analog of vitamin A, acts as a potent morphogen and as a teratogen during development, and either excess or reduced RA causes abnormal development in several organs in laboratory animals.[16] In humans, it has been reported that RA treatment given to pregnant women causes RA embryopathy, involving conotruncal heart defects and craniofacial malformations that closely resemble those observed in laboratory animals.[17] We previously reported that single-dose administration of all-*trans* RA to pregnant mice at embryonic day (ED) 8.5 caused TGA in embryos at an incidence of 80%.[6] Consequently, RA administered during a narrow window is capable of altering developmental processes, thereby inducing TGA morphology at cellular and molecular levels.[18,19]

To identify the region responsible for TGA in AHF or SHF, a single RA-soaked bead was implanted on the AHF or SHF at the early looped heart stage in chick (stages 12 to 14), and the incidence of TGA was examined at stage 34 (ED 8). TGA was found at high incidence in embryos in which an RA-soaked bead had been placed on left pharyngeal arches 1 and 2 (pha1/2) at stage 12. These results suggest that TGA is caused by impaired development of the left AHF at the early looped heart stage.

Methods

Chick Embryos

Fertilized eggs were incubated at 37°C and 70% humidity. After 42 to 48 hours of incubation, 4 mL of egg albumin was removed and a fenestration (1.5×2 cm) was made. To facilitate embryo visualization, 10% carbon ink (Platinum)/Tyrode's solution was injected into the yolk sac beneath the embryo, and staging according to Hamburger and Hamilton was performed.[20] Animal handling and procedures were performed in accordance with the guidelines of the Osaka City University animal care and use committee.

Bead Implantation in AHF or SHF

RA-soaked beads (all-*trans* RA, 0.25 to 0.5 mg/mL in dimethyl sulfoxide [Sigma-Aldrich]; AG1X-2 beads, citrate form, 100 μm in diameter [Bio-Rad]) were prepared, as described previously.[21] To expose the SHF to RA, the pericardial cavity was opened, and an RA-soaked bead (or control bead soaked in dimethyl sulfoxide) was placed on the visceral mesoderm of the pericardial coelom dorsal to the heart OFT (arrowhead in Figure S1). To expose the AHF to RA, an RA-soaked bead was placed on the left, on the right, on or both sides of the ventral pharyngeal ectoderm at the level of pha1/2 (arrow in Figure S1). Embryos were reincubated to appropriate stages and sacrificed, and hearts were fixed with 4% paraformaldehyde (PFA) in PBS and examined under a stereoscopic microscope.

Fluorescent Dye Tracing In Ovo

To trace the AHF in the second pharyngeal arch, stage 12 embryos were pressure injected with DiI (1,1′-dioctadecyl-3,3,3′,3′-tetramethyl-indocarbocyanine perchlorate) and DiO (3,3′-dioctadecyloxacarbocyanine perchlorate; Molecular Probes), as described previously.[14] DiI was pressure injected into the mesodermal core of right pharyngeal arch 2, and DiO was pressure injected into the left using a pulled glass capillary needle equipped with a pressure injector (Narishige), and then an RA-soaked bead was implanted as described above. To trace the cardiac neural crest (cNC) cells, cNC cells of stage 10 embryos were pressure injected with DiI or DiO. The embryo was reincubated and sacrificed at stage 27, and the heart was fixed with 4% PFA/PBS and examined under a stereoscopic fluorescent microscope. Hearts were fixed for an additional 12 hours at 4°C and embedded in optimal cutting temperature compound (Sakura). Frozen sections were cut and examined under a fluorescent microscope.

Organ Culture of Left AHF

Left second pharyngeal arch was extirpated from stage 12 embryos using an electromicrosurgery tool, Gastromaster (Nepagene). The resulting pharyngeal explants containing AHF were cultured in medium (75% DMEM, 25% McCoy's medium, 5% fetal bovine serum, and penicillin-streptomycin; Gibco) containing various concentrations of RA (10^{-7} to 10^{-5} mol/L) or dimethyl sulfoxide alone (control explants). Explants were cultured for 30 hours, fixed with 4% PFA/PBS, and subjected to immunostaining.

Fluorescence Microscopy

Pharyngeal regions were fixed in 4% PFA/PBS for 30 minutes at room temperature. After extensive washing in PBS, samples

were embedded in optimal cutting temperature compound and frozen in liquid nitrogen. Frozen sections were cut on a cryostat and mounted on slides. After being rinsed in PBS, sections were blocked with 1% BSA/PBS for 1 hour, incubated with a primary antibody for 12 hours at 4°C, rinsed with PBS, and then incubated with a secondary antibody for 2 hours at room temperature. Nuclei were stained with DAPI (4′,6-diamidino-2-phenylindole) for 20 minutes, rinsed with PBS, and mounted. Samples were observed under a conventional fluorescent microscope (Olympus). For phosphohistone H3 staining, sections were preincubated in 100% methanol for 5 minutes at −20°C, rinsed in PBST (PBS containing 0.1% Triton X-100) and 10 mmol/L citrate buffer (pH 6) for 30 minutes at 95°C before blocking.

Cultures were drained of medium, rinsed with PBS, fixed with 4% PFA/PBS for 1 hour at room temperature, and rinsed with PBS. Samples were blocked for 1 hour with 1% BSA/PBST and then incubated with the primary antibody mixture at 4°C overnight. Samples were rinsed with PBS and incubated with the secondary antibody mixture for 2 hours at room temperature. After extensive washing, they were mounted with mounting medium and observed under a conventional fluorescent microscope or laser confocal microscope (Leica).

Whole -Mount In Situ Hybridization

Digoxigenin-labeled single-strand RNA probes were prepared using a digoxigenin RNA labeling kit (Roche Diagnostics). To produce an antisense probe, chick *Fgf8b*/pGEM7 Zf (+) or chick *Pitx2*/pCS2 (+) were linearized using EcoRI or BamHI and transcribed using T7 RNA polymerase. Whole-mount in situ hybridizations were performed, as described previously.[22] Embryos were fixed in 4% PFA/PBS for 2 hours, rinsed with PBT (PBS containing 0.1% Tween 20), dehydrated and rehydrated through a graded series of methanol in PBT, digested with proteinase K (10 μg/mL), and refixed with 0.2% glutaraldehyde/4% PFA in PBT for 20 minutes. After rinsing with PBT, samples were prehybridized for 2 hours at 65°C and hybridized with digoxigenin-labeled probes in hybridization buffer for 12 hours at 65°C. After hybridization, samples were washed in 5× saline–sodium citrate/50% formamide/1% SDS for 1 hour at 65°C, 2× saline–sodium citrate/50% formamide for 1 hour at 65°C, rinsed with TBST (Tris-buffered saline containing 0.1% Tween 20), blocked with 20% sheep serum in TBST for 1 hour, and incubated with alkaline phosphatase–conjugated anti-digoxigenin antibody for 12 hours at 4°C. Hybridization was detected using NBT/BCIP (4-nitroblue tetrazolium chloride/5-bromo-4-chloro-3-indolyl-phosphate).

Image Analysis

Immunofluorescent images were taken with a CCD camera under the same conditions and analyzed by using the image analysis software Lumina Vision (Olympus). To examine the cellular polarity in AHF cells, a clockwise angle between the vector from the center of the nucleus to the GM130-positive Golgi and the right–left axis (0° to 180°) was measured, and the percentages of cell numbers in 12 angle ranges were plotted on a radar graph. In cultured explants, the distance (space) between Z-lines and the sarcomeric α-actinin–positive area (cardiomyocytes) were measured and compared between control and RA-treated explants. In anti-Isl1 antibody–stained sections, green fluorescence–positive nuclei (Isl1-positive nuclei) were extracted and counted in ventral pharyngeal ectoderm, mesoderm (AHF), and endoderm. Numbers of Isl 1-postitive cells were compared between left and right pharyngeal regions.

Statistical Analysis

Fisher's exact test was used to compare the incidences of heart defect between groups. The Mann–Whitney *U* test was used to compare the OFT lengths, Z-Z spaces, or α-actinin–positive areas between control and RA-treated samples. Bonferroni correction was used for multiple comparisons. The frequencies of vector-angle distribution (cellular polarity) in AHF cells were compared for 4 angle ranges (≤75°, ≤165°, ≤255°, and ≤345°) using the χ^2 test. Numbers of Isl1-positive cells were compared between left and right pharyngeal regions using the Wilcoxon signed-rank test. The significance level was set at <5%.

Antibodies

The antibodies used are presented in Table S1.

Results

RA-Induced TGA in Chick Embryos

To define the morphology of conotruncal heart defects, we examined hearts at stage 34 (ED 8), at which the interventricular septum is completed in normal development. Great arteries, atria, and ventricles were cut parallel to the surface of the atrioventricular valves. Resulting hearts were observed from the atrial and apical sides to determine the position of the great arteries and intraventricular morphology, respectively. In control hearts, the aortic valve was positioned in the right dorsal direction from the pulmonary valve (Figure 1A). Dextroposed aorta (DPA) was diagnosed if the semilunar valves were oriented side by side with the line passing the center of the semilunar valves parallel to that passing the posterior edge of atrioventricular valves (Figure 1B). TGA was defined as transposition of the aortic valve in the right ventral direction of the pulmonary valve, which was positioned close

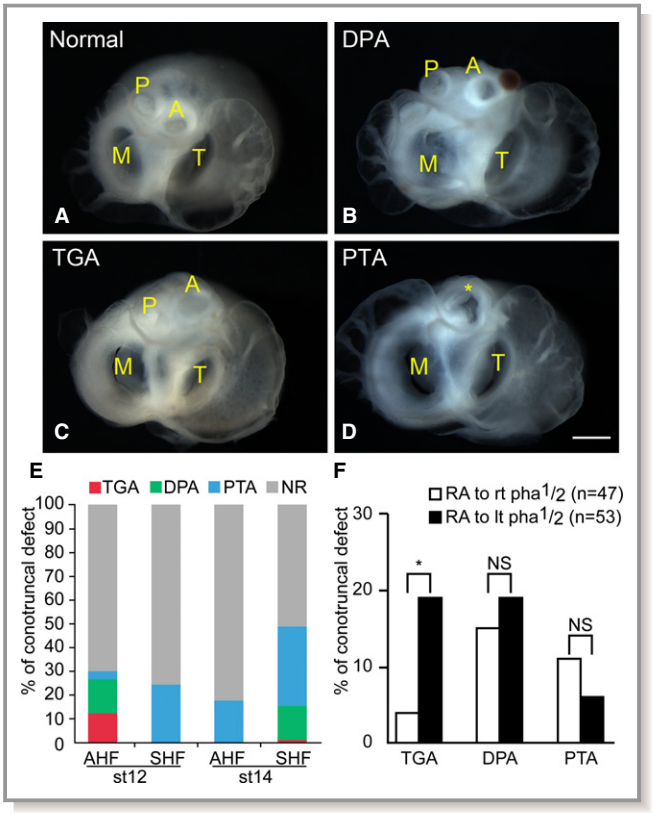

Figure 1. RA-soaked bead placed on left AHF caused TGA morphology. A through E, An RA-soaked (0.5 mg/mL) or control (dimethyl sulfoxide–soaked) bead was placed on AHF (pha1/2) or SHF (visceral mesoderm dorsal to the heart outflow tract) at stage 12 or 14. Embryos were reincubated and sacrificed at stage 34 (embryonic day 8), and conotruncal heart defects were inspected. Hearts viewed from the atrial side show a normal position of the great arteries (A), DPA (B), TGA (C), and PTA (D). When AHF was exposed to an RA-soaked bead at stage 12, TGA was diagnosed in 12% (4 of 34), DPA was diagnosed in 15% (5 of 34), and PTA was diagnosed in 3% (1 of 34). Neither TGA nor DPA was diagnosed if SHF was exposed to an RA-soaked bead at stage 12 (0 of 17) or AHF was exposed at stage 14 (0 of 17). RA-soaked beads placed on the left and right SHF at stage 14 induced PTA (33%, 9 of 27), DPA (15%, 4 of 27), and TGA (4%, 1 of 27) (E). The incidence of TGA/DPA was significantly high in the group of RA-exposed AHF at stage 12 versus RA-exposed SHF at stage 14 ($P<0.05$, Fisher's exact test). The incidence of TGA was significantly high when the left AHF was exposed to an RA-soaked bead (F; *$P<0.05$, Fisher's exact test). Bar, 500 μm. A indicates aorta; AHF, anterior heart field; DMSO, dimethyl sulfoxide; DPA, dextroposed aorta; lt, left; M, mitral valve; NR, normal; NS, no significant difference; P, pulmonary trunk; pha1/2, pharyngeal arches 1 and 2; PTA, persistent truncus arteriosus; RA, retinoic acid; rt, right; SHF, secondary heart field; st, stage; T, tricuspid valve; TGA, transposition of the great arteries.

to the mitral valve (Figure 1C). Persistent truncus arteriosus (PTA) was diagnosed if the common arterial trunk originated from the ventricle (Figure 1D). Large ventricular septal defect was observed in all hearts with DPA, TGA, or PTA (arrowheads in Figure S2).

To examine the spatiotemporal effect of RA on the AHF/SHF, a single RA-soaked bead was placed on both left and right AHF (or SHF) at stage 12 (16 to 18 somite stage) or stage 14 (20 to 22 somite stage); a mouse model of RA-induced TGA most frequently occurred when a single dose of RA was administered to pregnant mice at ED 8.5, at which the heart development of mouse embryo is equal to that of a stage 12 chick embryo.[23,24] To expose the AHF to RA, an RA-soaked bead was placed on the left and right ventral ectoderm at the level of pha1/2. When the left and right AHFs were treated with an RA-soaked bead (0.5 mg/mL) at stage 12, TGA, DPA, and PTA were diagnosed at 12% (4 of 34), 15% (5 of 34), and 3% (1 of 34), respectively (Figure 1E). When the left and right SHFs were exposed to an RA-soaked bead at stage 12, neither TGA nor DPA was found, whereas PTA was diagnosed at 24% (4 of 17) (Figure 1E). If both left and right AHFs were exposed to an RA-soaked bead at stage 14, neither TGA nor DPA was found, whereas PTA was diagnosed at 18% (3 of 17) (Figure 1E). RA-soaked beads placed on the left and right SHF at stage 14 induced PTA (33%, 9 of 27), DPA (15%, 4 of 27), and TGA (4%, 1 of 27) (Figure 1E). The incidence of TGA and DPA was significantly higher in the group with RA-exposed AHF at stage 12 than in those with RA-exposed SHF at stage 14, whereas PTA was significant in latter group ($P<0.05$, Fisher's exact test).

Mouse mutants with a deletion of the left–right asymmetrical gene are reported to be associated with TGA, suggesting that abnormal development of either left or right AHF may be responsible for TGA morphology.[25,26] Consequently, we examined whether the addition of an RA-soaked bead at the left or right AHF can cause TGA. An RA-soaked bead (0.25 to 0.5 mg/mL) was placed on the left or right pha1/2 at stages 12 to 13, and the resulting embryonic hearts were inspected at stage 34 (ED 8). The results showed that the incidence of TGA was significantly higher in hearts from embryos for which the RA bead was placed on left pha1/2 (19% [10 of 53] versus 4% [2 of 47], $P<0.05$, Fisher's exact test) (Figure 1F). There was no significant difference in the incidence of DPA or PTA between embryos treated on the left and right sides. The results indicate that the addition of RA to the left AHF at stage 12 effectively induces TGA.

RA-Exposed Left AHF Failed to Migrate to Conotruncus

We previously reported that proximal OFT is truncated in RA-induced TGA in mouse[8]; therefore, we next examined the length of proximal OFT (between the base and the top of the proximal OFT) in RA-bead–treated embryos. Stage 12 embryos implanted with RA-soaked beads (0.5 mg/mL) on both left and right AHFs were incubated, and the length of the proximal OFT was examined at stage 18 (ED 3) and

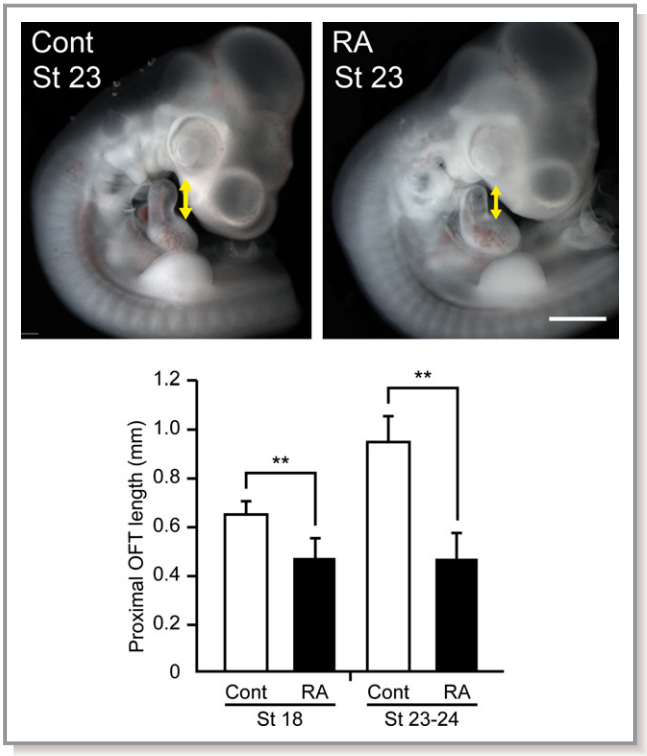

Figure 2. OFT is truncated in embryos treated with an RA-soaked bead. Stage 12 embryos in which an RA-soaked bead (0.5 mg/mL) or a control bead was placed at both left and right pharyngeal arches 1/2 were incubated, and the length of the proximal OFT was measured at stage 18 (5 control embryos, 8 RA-exposed embryos) and stages 23 to 24 (6 control embryos, 7 RA-exposed embryos). The length of the proximal OFT in embryos implanted with an RA-soaked bead was significantly shorter than that in control. Note that the length was measured between the base and the top of the proximal OFT (double arrow). $**P<0.01$ (Mann–Whitney *U* test). Bar, 1 mm. Cont indicates dimethyl sulfoxide–soaked bead; OFT, outflow tract; RA, retinoic-acid-soaked bead; St, stage.

stages 23 to 24 (ED 4). The results showed that the length of the proximal OFT was significantly shorter in RA-treated embryos than in controls (implanted with dimethyl sulfoxide-soaked beads) (Figure 2), suggesting that the elongation or growth of the OFT was affected in RA-treated chick embryos. We next examined whether ectopic RA exposure affected the migration or movement of cells from the left AHF to the conotruncus. An RA-soaked bead was placed in the left pha1/2, of which the mesenchymal core (containing AHF) had been labeled with DiO (green; right AHF was marked with DiI and had a control bead placed at it), reincubated, and observed at stage 27 (ED 5) under a fluorescent stereoscopic microscope. As reported previously, in control embryos, DiO-labeled cells from the left AHF migrate to the left side of the conotruncus (arrowhead in Figure 3A' and 3B'), and DiI-labeled cells from the right AHF migrate to the right side (arrow in Figure 3A' and 3B').[14] In embryos implanted with an RA-soaked bead (0.5 mg/mL) at the left AHF, DiI-labeled cells migrated to the right proximal OFT (arrow in Figure 3C' and 3D'), whereas DiO-labeled cells remained in the distal OFT and pharyngeal region (18 of 21) (arrowheads in Figure 3C' and 3E'). In addition, in RA-treated embryos, the OFT appeared to be straight and short, whereas OFT in the control heart elongated and formed flexion in the left ventral direction.

We next investigated the cellular polarity of AHF cells exposed to RA. An RA-soaked bead or control bead was placed on the left pha1/2 at stage 12 and reincubated for 6 hours. Resulting embryos were stained with anti-GM130 (marker for Golgi), and the cellular polarity of AHF cells was analyzed. We measured a clockwise angle between the vector from the center of the nucleus to the Golgi and the right–left axis (0° to 180°). In right AHF or a control bead placed left AHF, the vector angle was frequently distributed in 166° to 255° (Figure 4A and 4A') ($P<0.01$, χ^2 test) and 256° to 345° (Figure 4C and 4C') ($P<0.01$), respectively, whereas polarity of the vector angle was not significant in RA-treated left AHF (Figure 4B and 4B', $P=0.13$, χ^2 test). Results indicated that the cellular polarity was not apparent in RA-treated left AHF, suggesting that AHF cell migration was potentially affected in embryos treated with an RA-soaked bead.

The interaction between the cNC and AHF/SHF is important for normal OFT elongation and remodeling because myocardial addition to the arterial pole is perturbed in cNC–ablated chick embryonic heart[27]; therefore, we examined whether the cNC migration into OFT was affected when left AHF was exposed to an RA-soaked bead. In embryos treated with RA at the left AHF, the migration of cNC was not affected markedly, and the aorticopulmonary septum was generated in a manner similar to that of control embryos (Figure S3). Phosphohistone H3 detection (indicating M-phase) showed no significant difference in the mitotic index between control and RA-treated pharyngeal mesenchyme (Figure S4). Caspase-3–expressing cells (indicating apoptosis) were not found in control and RA-treated pharyngeal regions (not shown). These observations suggest that RA perturbed the migration of the heart progenitors in the AHF to the growing OFT.

RA Suppressed Cardiomyocyte Development From the AHF in Culture

To examine whether cardiomyocytes failed to descend in the RA-treated AHF, immunohistochemical detection of sarcomeric α-actinin was performed. Sarcomeric α-actinin was expressed in the myocardium of the OFT but not in the AHF in both control and RA-treated embryos (not shown), indicating that there was no ectopic accumulation of cardiomyocytes in RA-treated AHF. Consequently, we next

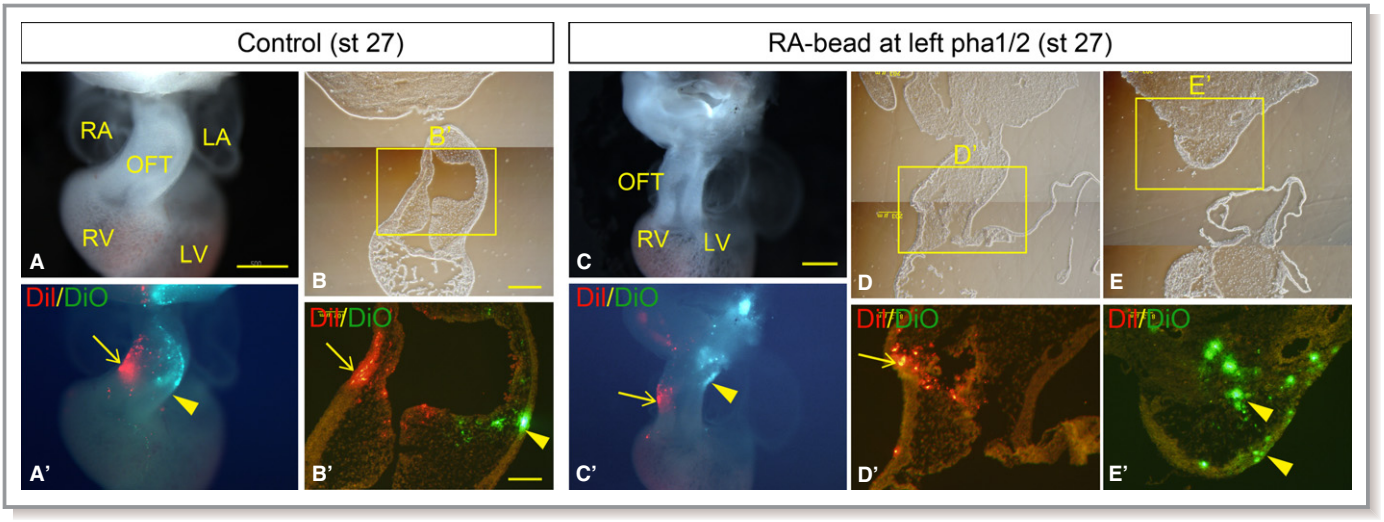

Figure 3. RA-exposed left AHF cells failed to migrate to the OFT. An RA-soaked bead was placed on the left pha1/2, of which the mesenchymal core (AHF) had been labeled with DiO (green). The right AHF was marked with DiI (red) and treated with a control bead. Embryos were observed at stage 27 (embryonic day 5) under a fluorescent stereoscopic microscope. In control embryos, DiO-labeled cells from the left AHF migrated to the left side of the conotruncus (arrowhead in A' and B') and DiI-labeled cells from the right AHF migrated to the right side (arrow in A' and B'). In embryos in which an RA-soaked bead (0.5 mg/mL) was placed on the left pha1/2 (AHF), DiI-labeled cells from the right AHF cells migrated to the right proximal OFT (arrow C' and D'), whereas DiO-labeled left AHF cells remained in the distal OFT and pharyngeal region (18 of 21; arrowheads in C' and E'). Bars, 500 μm (A, A' and C, C'); 250 μm (B, D, and E); 100 μm (B', D', and E'). AHF indicates anterior heart field; DiI, 1,1′-dioctadecyl-3,3,3′,3′-tetramethyl-indocarbocyanine perchlorate; DiO, 3,3′-dioctadecyloxacarbocyanine perchlorate; LA, left atrium; LV, left ventricle; OFT, outflow tract; pha1/2, pharyngeal arches 1 and 2; RA, retinoic acid; RV, right ventricle; st, stage.

examined whether RA could inhibit the differentiation of cardiomyocytes from the AHF. We cultured the left second pharyngeal arch that had been prepared from stage 12 embryos in medium supplemented with or without RA. In control explants, terminally differentiated cardiomyocytes with well-developed striation consisting of sarcomeric α-actinin were observed after 30 hours of incubation (Figure 5A and 5A'). In RA-treated AHF, sarcomeric α-actinin was deposited as a bead-like structure, indicating an immature state of myofibrillogenesis (Figure 5B and 5B').[28] To examine sarcomere maturation, we measured the space between sarcomeric α-actinin-positive
Z-lines. The space between Z-lines was significantly narrow in RA-treated explants in comparison with the control (Figure 5C). Furthermore, the sarcomeric α-actinin-positive area in RA-treated explants was significantly smaller than that in control explants (Figure 5A, 5B, and 5D). These results indicate that RA inhibited differentiation of cardiomyocytes from the progenitor pool in the AHF.

Isl1 Expression Was Suppressed in RA-Treated AHF

Heart-related transcription factors, which are required for heart specification and differentiation, play a role in the generation of the OFT from the AHF/SHF. Consequently, we next performed immunohistochemical detection of heart transcription factors including Isl1, Nkx2.5, and Gata4 in the AHF with or without RA treatment. An RA-soaked bead (0.5 mg/mL) or a control bead was placed on the left pha1/2 at stage 12 and reincubated for 6 hours, and the resulting embryos were examined at stage 14. In control embryos, nuclear localization of Isl1 staining was apparent in both left and right AHF (arrows in Figure 6A) and in pharyngeal ectoderm (arrowheads in Figure 6A), but no apparent staining was seen in the OFT myocardium (OFT in Figure 6A). In RA-bead–treated embryos, the number of Isl1-positive cells was reduced in the left AHF and its adjacent ectoderm (red arrow and arrowhead in Figure 6B and 6B') in comparison with those on the right side (yellow arrow and yellow arrowhead in Figure 6B and 6B'). There was no significant difference in the number of Isi1-positive cells between left and right pharyngeal regions in control embryos (Figure 6A'). In addition, when a RA bead was placed on the right pha1/2, the number of Isl1-positive cells was reduced in the right pharyngeal regions (Figure S6). Nkx2.5 was expressed in the AHF and in the myocardium of the OFT, and there was no apparent difference in the Nkx2.5 staining between controls (n=6) and RA-treated embryos (n=4) (Figure S7A and S7B). GATA4 was detected in the nuclei of OFT myocardium (arrowhead in Figure S7C and S7D) but was not detectable in the AHF (Figure S7C and S7D). There was no apparent difference in the deposition of GATA4 in the OFT myocardium between controls (n=3) and RA-treated embryos (n=5).

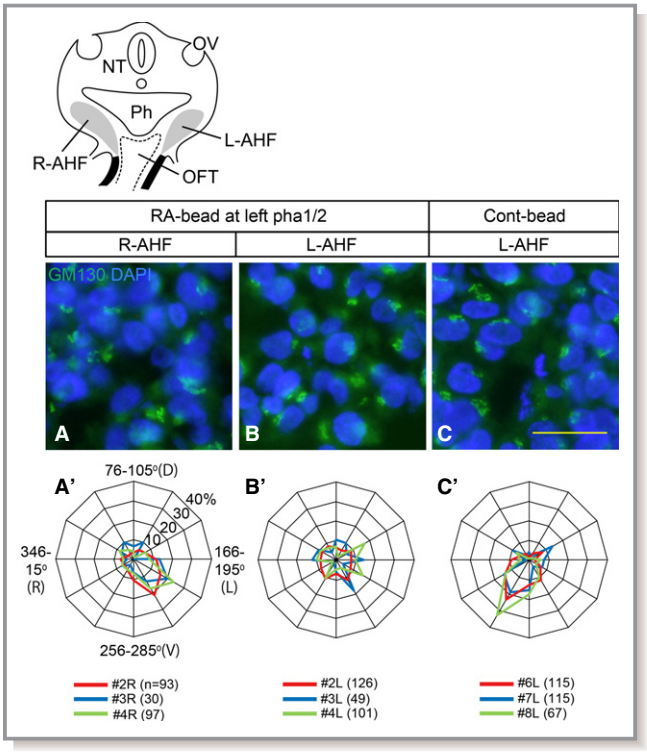

Figure 4. Cellular polarity was affected in RA-treated left AHF. Cellular polarity of AHF cells was examined. An RA-soaked bead or control bead was placed on left pha1/2 at stage 12 and reincubated for 6 hours, and the resulting embryos were stained with anti-GM130 (marker for Golgi). A clockwise angle between the vector from the center of nucleus to Golgi and right–left axis (0° to 180°) was measured in individual AHF cells. The percentage of cell number in each angle range was plotted on radar graphs, which showed a similar distribution pattern of data obtained from 3 embryos in each graph (A', R-AHF, P=0.91; B', RA-treated L-AHF, P=0.34; C, control L-AHF, P=0.051, χ^2 test). In the right AHF and control bead placed left AHF, the vector angle was frequently distributed in 166° to 255° (A', P<0.01) and 256° to 345° (C', P<0.01), respectively, whereas polarity of the vector angle was not significant in RA-treated left AHF (B', P=0.13, χ^2 test). Schematic drawing shows a cross-section of the second pharyngeal arch region containing the AHF. Bar, 25 μm. AHF indicates anterior heart field; Cont, dimethyl sulfoxide–soaked bead; L, left; n, number of cells examined; NT, neural tube; OFT, outflow tract; OV, otic vesicle; Ph, pharynx; pha1/2, pharyngeal arches 1 and 2; R, right; RA, retinoic acid.

It has been reported that loss of *Fgf8* expression in the AHF results in decreased expression of *Isl1* and causes alignment defect of the OFT, such as TGA and DPA.[29] In RA-treated embryos, the expression of *Fgf8* in left pharyngeal arch 2, in which an RA bead had been implanted, was downregulated in comparison with that observed in control-bead– treated embryos (arrow in Figure 7). Left–right asymmetry gene *Pitx2* also plays an important role in OFT development, and null mutant hearts show DPA and TGA.[26] We examined whether the expression of *Pitx2* was altered in

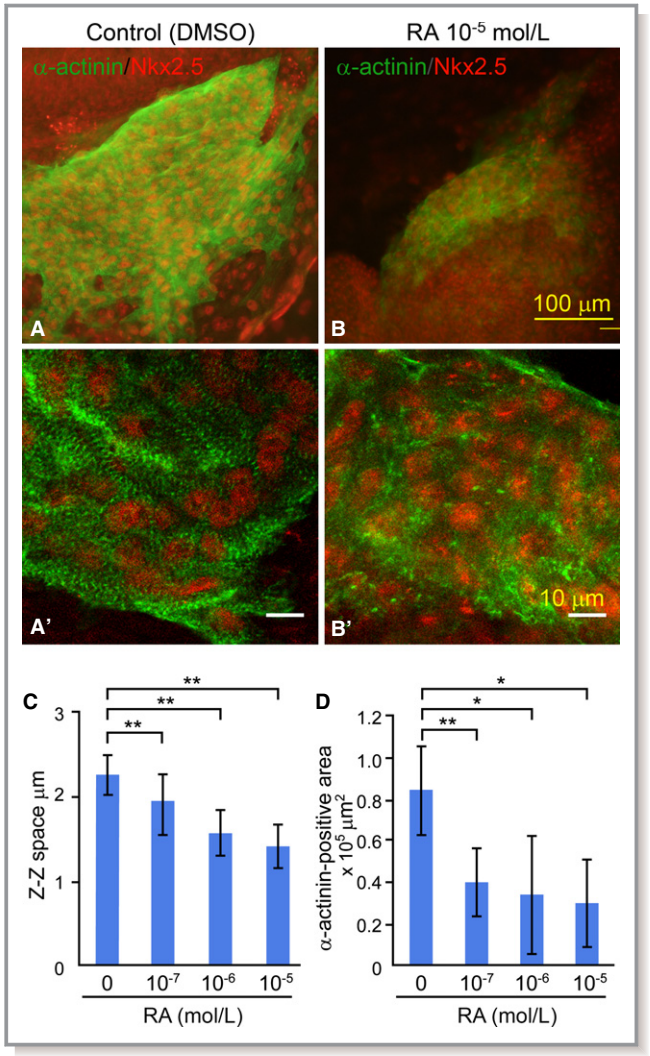

Figure 5. RA inhibits cardiomyocyte development in cultured left AHF. Left pharyngeal arch 2 was prepared from stage 12 embryos and cultured in medium supplemented with or without RA for 30 hours. Cultures were doubly stained with anti-sarcomeric α-actinin and anti-Nkx2.5 antibodies. In control cultures, terminally differentiated cardiomyocytes consisting of well-developed sarcomeric actinin-positive Z-bands were observed (A and A'), whereas in RA-treated cultures, there were immature cardiomyocytes consisting of premature Z-bands (bead-like deposition of sarcomeric α-actinin) (B and B'). The space between Z-bands (Z-bodies) in RA-treated explants (10^{-7} mol/L [4 explants, 1.92±0.33 μm], 10^{-6} mol/L [6 explants, 1.55±0.27], 10^{-5} mol/L [4 explants, 1.4±0.26]) was significantly narrow in comparison with that in the control (9 explants, 2.25±0.22) (C). The sarcomeric α-actinin/Nkx2.5-positive area in control explants (n=8, 0.82±0.25 $\mu m^2 \times 10^5$) (A and D) was significantly larger than that in RA-treated explants (10^{-7} mol/L [n=8, 0.4±0.17 μm^2], 10^{-6} mol/L [n=8, 0.34±0.29], 10^{-5} mol/L [n=4, 0.30±0.21]) (B and D). A and B, conventional fluorescent microscopic images; A' and B', confocal microscopic images; *P<0.05; **P<0.01 (Mann–Whitney U test after Bonferroni correction). AHF indicates anterior heart field; DMSO, dimethyl sulfoxide; RA, retinoic acid.

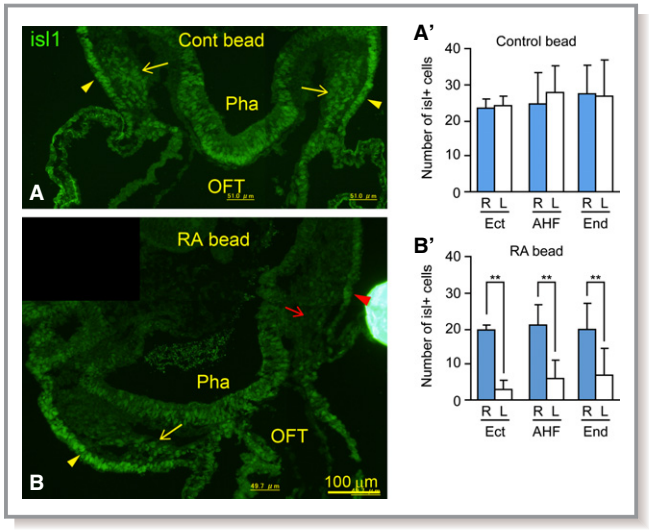

Figure 6. Isl1-positive cells were decreased in the left pharyngeal region treated with an RA-soaked bead. An RA-soaked (0.5 mg/mL) or dimethyl sulfoxide–soaked (control) bead was placed on the ectoderm of left pharyngeal arches 1/2 of stage 12 embryo. After 6 hours of reincubation, stage 14 embryos were sacrificed and stained with anti-Isl1 antibody. In control embryos, there was no significant difference in the number of Isl1-positive cells between left and right pharyngeal regions (A and A'; 5 sections from 4 embryos). In contrast, the number Isl1-positive cells in left pharyngeal ectoderm (red arrowhead), AHF (red arrow), or endoderm was significantly decreased in embryos treated with an RA-soaked bead (B and B'; 9 sections from 5 embryos). Note that (A and B) were constructed from 2 photographs obtained with a ×20 objective lens (photographs obtained at ×10 are shown in Figure S5). $**P<0.01$ (Wilcoxon signed rank test). AHF indicates anterior heart field; Cont, control; Ect, pharyngeal ectoderm; End, pharyngeal endoderm; L, left; OFT, heart outflow tract; Pha, pharynx; R, right; RA, retinoic acid.

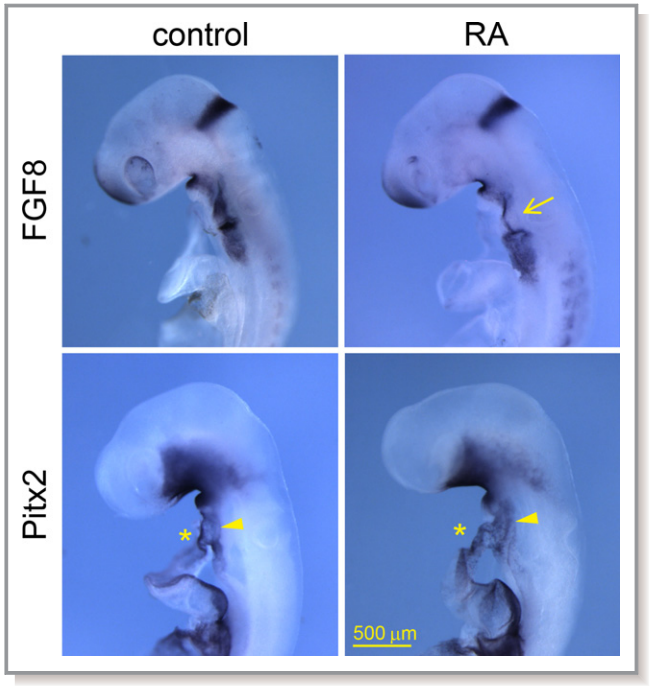

Figure 7. Fgf8 was downregulated in RA-treated AHF. Stage 12 embryos were treated with RA (or control) bead at left pharyngeal arches 1 and 2, reincubated, and sacrificed at stage 14 to 15, and the expression of *Fgf8* and *Pitx2* were examined. In control embryos, *Fgf8* was expressed in left and right pharyngeal regions, in which AHF/SHF resides. In RA-treated embryos, the expression of *Fgf8* was downregulated in the left AHF, especially in pharyngeal arch 2 (arrow), on which the RA-soaked bead had been placed. *Pitx2* was expressed in left splanchnic mesoderm (arrowheads) and left side of the OFT (*) in both control and RA-exposed embryos. There was no apparent difference in the expression of *Pitx2* between control and RA-treated pharyngeal region/OFT. Note that several embryos are shown in Figure S8. AHF indicates anterior heart field; OFT, heart outflow tract; RA, retinoic acid; SHF, secondary heart field.

RA-bead–treated embryos and found that the expression of *Pitx2* was not altered in left splanchnic mesoderm and OFT (arrowhead and * in Figure 7) in RA-exposed embryos.

Several signaling pathways are known to regulate cardiogenesis.[30] We performed immunohistochemical detection for growth factor–regulated signaling pathways including BMP (phospho-Smad1/5/8), TGF-β/Nodal (phospho-Smad2/3), and Wnt (β-catenin) in the AHF, for which a control bead (dimethyl sulfoxide) or an RA-soaked bead (0.5 mg/mL) was placed at the left pha1/2 at stage 12 (Figure S9). There was no apparent difference in the deposition of the above signaling molecules between control and RA-treated AHF.

Discussion

Impaired Development of Left AHF at Early Looped Heart Stage Causes TGA

We showed that a single RA-soaked bead placed on the left AHF (in pha1/2) of stage 12 embryos causes TGA in a spatiotemporally restricted manner. It has been reported that heart progenitors from the AHF or SHF are added to the arterial pole of the early looped heart to form conotruncus and right ventricle.[11–13] A fluorescent dye–tracing experiment showed that heart progenitors in either the left or the right AHF (or SHF) contribute to the distinct conotruncal regions.[14] These observations suggest that altered development of the particular region of the AHF or SHF at a particular stage may lead to a specific spectrum of conotruncal heart defects.[15] The cNC cells, which reside in the cephalic neural crest at the level of rhombomere 6 to somite 3, migrate to the arterial pole through pharyngeal arches 3 to 6 and provide smooth muscle cells of the pharyngeal arch artery derivatives and aorticopulmonary septum.[31] Surgical ablation of the cNC at the level of pharyngeal arches 3 to 6 causes PTA and DPA, but ablation at the level of pha1/2 leads only to DPA, suggesting the direct result of reduced cNC cells for PTA but a secondary

effect for DPA.[32] The primary cause of DPA in cNC–ablated embryos is the failure of myocardial addition to the OFT from the AHF or SHF.[27] In cNC–ablated embryos, TGA was not found, suggesting that TGA morphology could not be caused by a reduction of migrated cNC cells into the pharyngeal arches and OFT.[33] Another experiment showed that pulsed nitrogen dye laser ablation of chick embryo right SHF, which rotationally migrates to contribute to the left dorsal side of the OFT, causes overriding aorta associated with pulmonary stenosis or atresia (tetralogy of Fallot) as well as DPA.[34] In the present study, local administration at stage 12 of RA to the left AHF, which later migrates to form ventral wall of the right ventricular OFT close to the pulmonary valve, effectively induced TGA morphology. Neither RA-soaked bead implantation to the left AHF of stage 14 embryos nor RA-soaked bead implantation to the stage 12 SHF induced TGA morphology. Consequently, it is plausible that the left AHF at stage 12 is the region of the impediment that leads to TGA morphology; however, RA to the SHF at stage 14 also induced DPA/TGA, suggesting that the failure of cardiomyocyte addition from the SHF induces rotational defect at a relatively low extent. In a mouse model of TGA induced by single-dose administration of RA at ED 8.5, it was shown that TGA was induced in >80% of fetuses with normal visceral situs.[6,24] The developmental stage of heart (early looped heart) or pharyngeal arches (2 arches) in stage 12 chick embryo is equal to that in ED 8.5 mouse embryos,[23] suggesting that the critical stage responsible for causing TGA in situs solitus embryo is likely to be stage 12 in chick and ED 8.5 in mouse; such stages correspond to Carnegie stages 10 to 11 (28 to 29 days after fertilization) in human embryos.[35,36] Taken together with these observations, altered or abnormal development of the left AHF that occurs at the early looped heart stage may be an embryological cause of TGA.

Mechanics Leading to TGA

We showed that RA inhibited not only the migration of AHF to the conotruncal region in vivo but also the differentiation and expansion of cardiomyocytes in vitro. We previously reported that the left AHF in the pharyngeal arches migrates to establish the ventral myocardium of the right ventricular OFT close to the pulmonary valve.[14] In human embryonic heart with TGA or DPA, defective counterclockwise rotation of the OFT (viewed from the apex) appears to generate TGA morphology as well as great arteries oriented side by side.[5] Transgenic mouse, in which subpulmonic myocardium was marked, revealed that the marked left AHF migrates rotationally to form the subpulmonic myocardium. *Pitx2c* mutant mouse is highly associated with TGA and showed defective rotational movement of the subpulmonic myocardium during conotruncal development, suggesting that the failure of rotational movement of the subpulmonic myocardium is related to TGA morphology.[9] A 3-dimensional reconstruction study showed that the subpulmonic myocardium from the AHF pushes the right ventricular OFT and pulmonary orifice to a higher and more ventral position relative to the aortic orifice, and the failure of this process due to reduced cardiomyocyte addition from the AHF in VEGF120/120 mutant causes DPA.[37] Taking these observations and ours together, it is suggested that the defective addition of subpulmonic myocardium from the left AHF to conotruncus causes arrest or reduction of ventral movement of the pulmonary route relative to the aorta (ie, reduced counterclockwise rotation of the OFT viewed from the apex), resulting in DPA or TGA.

In RA-induced TGA in mouse, not only truncated OFT but also hypoplasia of the proximal region of parietal and septal ridges was shown.[6,8] In the normal OFT septation process, the parietal ridge that develops on the right side of the OFT fuses with the septal ridge to establish the spirally oriented outflow channels, namely, the left ventrally positioned pulmonary route and the right dorsally oriented aortic route. In RA-induced TGA in mouse, hypoplasia of the proximal part of these cushion ridges fails to establish the spirally oriented normal outflow channels; instead, distal cushion ridges that develop in a dorsal-ventral direction fuse to generate straight conotruncal septation, resulting in the parallel outflow channels.[7,8] Because some endothelial/mesenchymal cells in the OFT are derived from the AHF,[14,38] it is suggested that impaired development of the AHF would cause hypoplastic cushion ridges in the developing OFT. Given these observations, it is strongly suggested that truncated OFT, rotational defect of the OFT, and hypoplastic proximal cushion ridges are the morphological etiologies causing TGA morphology.

RA Affects Cardiomyocyte Development From the AHF

The expression of FGF8 and Isl1 was suppressed in the RA-treated AHF, from which dye-labeled heart progenitors failed to contribute to the developing OFT. In mouse, *Fgf8* and *Isl1* are expressed in the heart progenitors that reside in the AHF and regulate cell survival, proliferation, and migration of the AHF to involve the developing OFT; therefore, truncated OFT is observed in both the *Fgf8*-deficient mouse and the *Isl1*-null mutant.[29] In our experiment, RA-soaked bead treatment affected neither mitotic index nor apoptosis in the AHF, but it perturbed cellular polarity of AHF cells and OFT elongation. Furthermore, RA inhibited the differentiation and expansion of cardiomyocytes from cultured AHF. Consequently, it is suggested that RA treatment inhibited the expression of FGF8 and Isl1, and thus AHF cells failed to migrate and differentiate to OFT cardiomyocytes, which later contribute to elongation and septation of developing conotruncus. RA is a

potent morphogen regulating the anterior–posterior (cranio-caudal) axis of developing organs including heart and is synthesized by retinal dehydrogenase 2 (Raldh2) that is expressed in the mesoderm posterior (caudal) to the presomitic mesoderm, whereas RA-catabolizing enzyme Cyp26 is expressed in the cranial region; therefore, a minimum amount of endogenous RA acts on the AHF.[16,39,40] In *Raldh2*-null mutant mouse, the expression of *Fgf8* and *Isl1* expands to the posterior region of splanchnic mesoderm (posterior region of the SHF), in which the synthesis of endogenous RA is deleted, suggesting that RA signaling negatively controls the expression of *Fgf8* and *Isl1* to define the boundary of the AHF.[40] In zebrafish, RA induces the expression of the LIM domain protein Ajuba (a member of the Ajuba/Zyxin protein family), which binds to Isl1 to repress its expression, resulting in the suppression of cardiomyocyte differentiation and migration from the AHF or SHF, suggesting that proper cardiac morphogenesis is regulated, at least in part, by RA signaling.[41] In conclusion, the application of excess RA to the left AHF at the early looped heart stage affects the contribution of heart progenitors to OFT development, resulting in conotruncal heart defects such as TGA and DPA and suggesting that left AHF at the early looped heart stage is the region of the impediment that causes TGA morphology in situs solitus heart.

Limitations

In this study, we reported a chick model of TGA that was induced by RA administration to the AHF at early looped-heart stage. The number of embryos we examined was small because in ovo manipulations, including RA-bead implantation and fluorescent dye labeling, showed a low survival rate (≈30% at ED 8). This may suggest a potential limitation of this study. However, experiments showed that TGA was effectively induced in embryos that had been treated with local administration of RA at the left AHF at stages 12 to 13, and migration and differentiation of RA-treated AHF cells were affected. These results suggest that impaired development of left AHF cells at the early looped heart stage may be a cause of TGA morphology.

Sources of Funding

This work was supported by Japan Society for the Promotion of Science (JSPS) Grant-in-Aid for Scientific Research (C) 25460273.

Acknowledgment

The authors thank S. Uoya for preparing the manuscript.

Disclosures

None.

References

1. Hoffman JI, Kaplan S. The incidence of congenital heart disease. *J Am Coll Cardiol*. 2002;39:1890–1900.
2. Ferencz C, Brenner JI, Loffredo C, Kappetein AP, Wilson PD. Transposition of the great arteries: etiologic distinctions of outflow tract defects in a case control study of risk factors. In: Clark EB, Markwald RR, Takao A, eds. *Developmental Mechanisms of Heart Disease*. New York, NY: Futura Publishing; 1995:639–653.
3. Unolt M, Putotto C, Silvestri LM, Marino D, Scarabotti A, Valerio M, Caiaro A, Versacci P, Marino B. Transposition of great arteries: new insights into the pathogenesis. *Front Pediatr*. 2013;1:11.
4. Bostrom MP, Hutchins GM. Arrested rotation of the outflow tract may explain double-outlet right ventricle. *Circulation*. 1988;77:1258–1265.
5. Lomonico MP, Bostrom MP, Moore GW, Hutchins GM. Arrested rotation of the outflow tract may explain tetralogy of Fallot and transposition of the great arteries. *Pediatr Pathol*. 1988;8:267–281.
6. Yasui H, Nakazawa M, Morishima M, Miyagawa-Tomita S, Momma K. Morphological observations on the pathogenetic process of transposition of the great arteries induced by retinoic acid in mice. *Circulation*. 1995;91:2478–2486.
7. Yasui H, Nakazawa M, Morishima M, Ando M, Takao A, Aikawa E. Cardiac outflow tract septation process in the mouse model of transposition of the great arteries. *Teratology*. 1997;55:353–363.
8. Nakajima Y, Hiruma T, Nakazawa M, Morishima M. Hypoplasia of cushion ridges in the proximal outflow tract elicits formation of a right ventricle-to-aortic route in retinoic acid-induced complete transposition of the great arteries in the mouse: scanning electron microscopic observations of corrosion cast models. *Anat Rec*. 1996;245:76–82.
9. Bajolle F, Zaffran S, Kelly RG, Hadchouel J, Bonnet D, Brown NA, Buckingham ME. Rotation of the myocardial wall of the outflow tract is implicated in the normal positioning of the great arteries. *Circ Res*. 2006;98:421–428.
10. Gruber PJ, Epstein JA. Development gone awry: congenital heart disease. *Circ Res*. 2004;94:273–283.
11. Mjaatvedt CH, Nakaoka T, Moreno-Rodriguez R, Norris RA, Kern MJ, Eisenberg CA, Turner D, Markwald RR. The outflow tract of the heart is recruited from a novel heart-forming field. *Dev Biol*. 2001;238:97–109.
12. Waldo KL, Kumiski DH, Wallis KT, Stadt HA, Hutson MR, Platt DH, Kirby ML. Conotruncal myocardium arises from a secondary heart field. *Development*. 2001;128:3179–3188.
13. Kelly RG, Brown NA, Buckingham ME. The arterial pole of the mouse heart forms from Fgf10-expressing cells in pharyngeal mesoderm. *Dev Cell*. 2001;1:435–440.
14. Takahashi M, Terasako Y, Yanagawa N, Kai M, Yamagishi T, Nakajima Y. Myocardial progenitors in the pharyngeal regions migrate to distinct conotruncal regions. *Dev Dyn*. 2012;241:284–293.
15. Nakajima Y. Second lineage of heart forming region provides new understanding of conotruncal heart defects. *Congenit Anom (Kyoto)*. 2010;50:8–14.
16. Rhinn M, Dolle P. Retinoic acid signalling during development. *Development*. 2012;139:843–858.
17. Lammer EJ, Chen DT, Hoar RM, Agnish ND, Benke PJ, Braun JT, Curry CJ, Fernhoff PM, Grix AW Jr, Lott IT, Richard JM, Sun SC. Retinoic acid embryopathy. *N Engl J Med*. 1985;313:837–841.
18. Nakajima Y, Morishima M, Nakazawa M, Momma K. Inhibition of outflow cushion mesenchyme formation in retinoic acid-induced complete transposition of the great arteries. *Cardiovasc Res*. 1996;31:E77–E85.
19. Sakabe M, Kokubo H, Nakajima Y, Saga Y. Ectopic retinoic acid signaling affects outflow tract cushion development through suppression of the myocardial Tbx2-Tgfbeta2 pathway. *Development*. 2012;139:385–395.
20. Hamburger V, Hamilton HL. A series of normal stages in the development of the chick embryo. *J Morphol*. 1951;88:49–92.
21. Wang G, Scott SA. Retinoid signaling is involved in governing the waiting period for axons in chick hindlimb. *Dev Biol*. 2008;321:216–226.
22. Yamagishi T, Ando K, Nakamura H, Nakajima Y. Expression of the Tgfβ2 gene during chick embryogenesis. *Anat Rec*. 2012;295:257–267.
23. Sissman NJ. Developmental landmarks in cardiac morphogenesis: comparative chronology. *Am J Cardiol*. 1970;25:141–148.
24. Irie K, Ando M, Takao A. All-trans retinotic acid induced cardiac malformations. *Ann N Y Acad Sci*. 1990;588:387–388.

25. Liu C, Liu W, Palie J, Lu MF, Brown NA, Martin JF. Pitx2c patterns anterior myocardium and aortic arch vessels and is required for local cell movement into atrioventricular cushions. *Development*. 2002;129:5081–5091.
26. Ai D, Liu W, Ma L, Dong F, Lu MF, Wang D, Verzi MP, Cai C, Gage PJ, Evans S, Black BL, Brown NA, Martin JF. Pitx2 regulates cardiac left-right asymmetry by patterning second cardiac lineage-derived myocardium. *Dev Biol*. 2006;296:437–449.
27. Waldo KL, Hutson MR, Stadt HA, Zdanowicz M, Zdanowicz J, Kirby ML. Cardiac neural crest is necessary for normal addition of the myocardium to the arterial pole from the secondary heart field. *Dev Biol*. 2005;281:66–77.
28. Takahashi M, Yamagishi T, Narematsu M, Kamimura T, Kai M, Nakajima Y. The epicardium is required for sarcomeric maturation and cardiomyocyte growth in the ventricular compact layer mediated by TGFβ and FGF before the onset of coronary circulation. *Congenit Anom (Kyoto)*. 2014;54:162–171.
29. Park EJ, Ogden LA, Talbot A, Evans S, Cai CL, Black BL, Frank DU, Moon AM. Required, tissue-specific roles for Fgf8 in outflow tract formation and remodeling. *Development*. 2006;133:2419–2433.
30. Nakajima Y, Sakabe M, Matsui H, Sakata H, Yanagawa N, Yamagishi T. Heart development before beating. *Anat Sci Int*. 2009;84:67–76.
31. Kirby ML, Gale TF, Stewart DE. Neural crest cells contribute to normal aorticopulmonary septation. *Science*. 1983;220:1059–1061.
32. Nishibatake M, Kirby ML, Van Mierop LH. Pathogenesis of persistent truncus arteriosus and dextroposed aorta in the chick embryo after neural crest ablation. *Circulation*. 1987;75:255–264.
33. Kirby ML. Embryogenesis of transposition of the great arteries: a lesson from the heart. *Circ Res*. 2002;91:87–89.
34. Ward C, Stadt H, Hutson M, Kirby ML. Ablation of the secondary heart field leads to tetralogy of Fallot and pulmonary atresia. *Dev Biol*. 2005;284:72–83.
35. Kaufmann MH. *The Atlas of Mouse Development. General Observation on the Stages of Postimplantation Mouse Embryos*. Tokyo: Elsevier; 2008:5.
36. O'Rahilly R, Müller F. *Human Embryology and Teratology*. New York, NY: A John Wiley & Sons, Inc; 2001:89.
37. Scherptong RW, Jongbloed MR, Wisse LJ, Vicente-Steijn R, Bartelings MM, Poelmann RE, Schalij MJ, Gittenberger-De Groot AC. Morphogenesis of outflow tract rotation during cardiac development: the pulmonary push concept. *Dev Dyn*. 2012;241:1413–1422.
38. Cai CL, Liang X, Shi Y, Chu PH, Pfaff SL, Chen J, Evans S. Isl1 identifies a cardiac progenitor population that proliferates prior to differentiation and contributes a majority of cells to the heart. *Dev Cell*. 2003;5:877–889.
39. Okano J, Udagawa J, Shiota K. Roles of retinoic acid signaling in normal and abnormal development of the palate and tongue. *Congenit Anom (Kyoto)*. 2014;54:69–76.
40. Sirbu IO, Zhao X, Duester G. Retinoic acid controls heart anteroposterior patterning by down-regulating Isl1 through the Fgf8 pathway. *Dev Dyn*. 2008;237:1627–1635.
41. Witzel HR, Jungblut B, Choe CP, Crump JG, Braun T, Dobreva G. The LIM protein Ajuba restricts the second heart field progenitor pool by regulating Isl1 activity. *Dev Cell*. 2012;23:58–70.